

See discussions, stats, and author profiles for this publication at: <https://www.researchgate.net/publication/272144063>

Surface Termination of the Metal–Organic Framework HKUST–1: A Theoretical Investigation

ARTICLE *in* JOURNAL OF PHYSICAL CHEMISTRY LETTERS · SEPTEMBER 2014

Impact Factor: 7.46 · DOI: 10.1021/jz5012065

CITATIONS

7

READS

172

3 AUTHORS:



Saeed Amirjalayer

University of Amsterdam

39 PUBLICATIONS 602 CITATIONS

SEE PROFILE



Maxim Tafipolski

University of Wuerzburg

42 PUBLICATIONS 1,089 CITATIONS

SEE PROFILE



Rochus Schmid

Ruhr-Universität Bochum

77 PUBLICATIONS 2,037 CITATIONS

SEE PROFILE

Surface Termination of the Metal-Organic Framework HKUST-1: A Theoretical Investigation

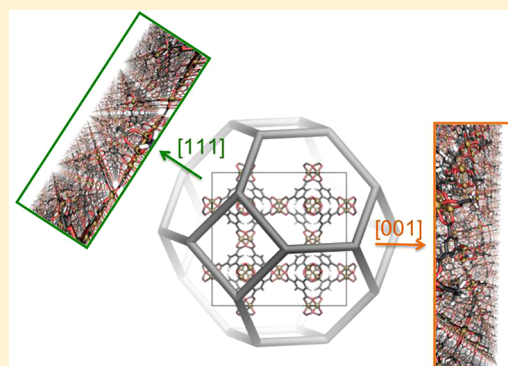
Saeed Amirjalayer,[†] Maxim Tafipolsky,[‡] and Rochus Schmid*

Lehrstuhl für Anorganische Chemie II, Organometallics and Materials Chemistry, Ruhr-Universität Bochum, Universitätsstr. 150, 44780 Bochum, Germany

Supporting Information

ABSTRACT: The surface morphology and termination of metal-organic frameworks (MOF) is of critical importance in many applications, but the surface properties of these soft materials are conceptually different from those of other materials like metal or oxide surfaces. Up to now, experimental investigations are scarce and theoretical simulations have focused on the bulk properties. The possible surface structure of the archetypal MOF HKUST-1 is investigated by a first-principles derived force field in combination with DFT calculations of model systems. The computed surface energies correctly predict the [111] surface to be most stable and allow us to obtain an unprecedented atomistic picture of the surface termination. Entropic factors are identified to determine the preferred surface termination and to be the driving force for the MOF growth. On the basis of this, reported strategies like employing “modulators” during the synthesis to tailor the crystal morphology are discussed.

SECTION: Surfaces, Interfaces, Porous Materials, and Catalysis



Porous coordination polymers, also referred to as “metal-organic frameworks” (MOFs), are a class of porous crystalline materials with fascinating properties like tunable pore space and network flexibility, making them potentially useful in various applications from gas storage, separation, to sensing and catalysis.^{1–3} Naturally, the main focus of both experimental and theoretical research in this field is on structure and properties of the bulk materials. However, the surface represents the most relevant “defect” of a crystalline bulk material. Understanding its atomistic structure is closely related to questions of interfacing and oriented growth for example in membrane applications^{4,5} and also to fundamental aspects of MOF growth and decompositions mechanism. Note that long-term stability is a primary issue for technical application.⁶

Only recently have some efforts been initiated to study the surfaces of MOFs.⁷ The most investigated system in this context is the copper paddle-wheel-based HKUST-1 ($\text{Cu}_3(\text{btc})_2$; $\text{btc} = 1,3,5\text{-benzenetricarboxylate}$) shown in Figure 1.⁸ In particular, an oriented growth on functionalized thiol self-assembled monolayers (SAMs) was observed under solvothermal growth conditions, with the [001] surface forming on carboxylate terminated layers and the [111] interface adhering to OH-terminated SAMs (see Figure 1).⁹ In the alternative layer-by-layer (lbl) growth mode, developed recently by Wöll and Fischer,¹⁰ smooth and thin MOF films are formed with the same growth orientation. Interestingly, in this case, the formation of the MOF is observed already at room temperature

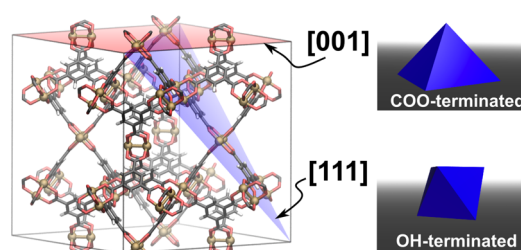


Figure 1. Unit cell of HKUST-1 showing the [001] and [111] crystal planes (left) and a schematic picture of the corresponding observed crystal morphology on functionalized thiol-SAMs (right).

if the acetate precursor $\text{Cu}_2(\text{ac})_4$ ($\text{ac} = \text{CH}_3\text{CO}_2$) was employed, which is already a dimer, whereas the monomeric nitrate precursor $\text{Cu}(\text{NO}_3)_2$ is active only at higher temperatures in the solvothermal mode.¹¹ In these cases, the morphology of HKUST-1 crystals is octahedral, indicating a preference for an increased stability of the [111] surface. However, Furukawa and coworkers found cubic crystals when using long-chain monocarboxylic growth modulators.¹² A further important observation, which was made during both in situ AFM measurements and lbl synthesis of HKUST-1 films, is the fact that always half a unit cell is grown at once, which

Received: June 12, 2014

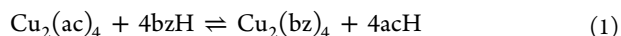
Accepted: August 31, 2014

Published: September 1, 2014

implies the incorporation of two “layers” of copper dimers in one growth step.^{9,10,13–22}

To the best of our knowledge, this is the first attempt to tackle the problem of surface termination and the connected growth mechanism of a MOF by theoretical methods.⁷ A combination of quantum mechanics (QM) calculations of model systems and molecular mechanics (MM) calculations using a QM-adjusted parametrization can be used to determine relative surface formation energies for a slab model. Corresponding free energies can be derived by a thermodynamic approach²³ using the chemical potential of a reservoir of monomeric building units. We employ here our first-principles-derived force field for copper paddle-wheel systems. The parametrization procedure and force-field validation has been described in detail in ref 24. The force field is able to describe the structure and dynamics of HKUST-1, including a quantitative representation of the negative thermal expansion, which involves both local and global internal vibrations.²⁴ In addition, it can be used for structural prediction of deformed frameworks.²⁵ On the basis of this, we use it to relax the atomistic structure for different surface terminations and to quantify its strain effects. The computational methodology of our approach is explained in full detail in the Supporting Information (SI) together with the employed force-field terms and parameters.

The formation of HKUST-1 already occurs at ambient temperatures in the *lbl* mode from the dimeric acetate precursor $\text{Cu}_2(\text{ac})_4$.^{10,11} This means, the acetate (*ac*) is replaced (presumably in a proton-catalyzed exchange reaction) by the aromatic carboxylate linker *btc*. To analyze the thermodynamics of this process, we first computed isodesmic reaction energies for the model reaction replacing *ac* by benzoate (*bz*)



With a reaction energy of $\Delta H_{\text{R}} = -0.61$ kcal/mol (including zero-point energy, thermal contributions at $T = 298.15$ K), the exchange is (almost) energetically neutral. This value is only slightly changed by including solvation effects using the CPCM method^{26,27} (solvent ethanol) to $\Delta H_{\text{R,solv.}} = -0.84$ kcal/mol. Thus, also the formation of HKUST-1 from H_3btc and the $\text{Cu}_2(\text{ac})_4$ precursor should be nearly thermoneutral from an enthalpic point of view. In contrast with that the entropy increases significantly due to the release of six acetate molecules upon the formation of one formula unit $\text{Cu}_3(\text{btc})_2$, indicating that the framework formation is mainly an entropy-driven process when starting from the $\text{Cu}_2(\text{ac})_4$ precursor. In this context, it is important to note that for the surface chemistry of hard materials like oxides or semiconductors dangling bonds and a corresponding surface reconstruction are usually observed.²⁸ Recently, an attempt was made to model the surface of the carboxylate-based MOF-5 by breaking the C–C bond between the phenyl and the carboxylate groups, which leads to a completely unphysical surface state.²⁹ However, in the case of MOFs, grown under solvothermal conditions, this will never be the case. Instead, always the weakest coordination bonds will be broken and the resulting free coordination sites will be blocked by donating ligands. It is plausible that the surface of HKUST-1 is terminated preferentially by not yet substituted acetate groups. The alternative would be a termination with partially reacted *btc* linkers, but results from infrared reflection absorption spectroscopy (IRRAS) of surface

grown HKUST-1 gave no evidence for free –COOH groups on the surface.³⁰

For the computation of surface energies, the following strategy was employed: From the 3D periodic system, a 2D periodic slab was generated by slicing all Cu–O bonds in a specific *hkl* plane. This results in the first place in two different surfaces, one with Cu_2 -dimers and one with “dangling” CO_2 groups exposed. To saturate these dangling bonds and to generate two identical surfaces, fragments from a reservoir of $\text{Cu}_2(\text{ac})_4$ molecular precursors are used (shaded red in Figure 2). Depending on the slicing, a different number of these

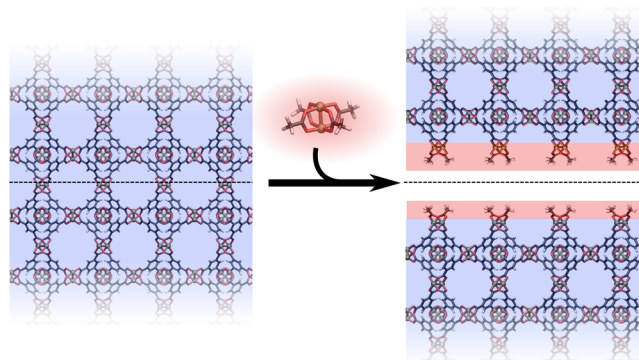


Figure 2. Isodesmic slicing reaction: generation of two identical acetate terminated surfaces by slicing of the bulk HKUST-1 and saturating all dangling bonds with groups taken from a reservoir of $\text{Cu}_2(\text{ac})_4$ precursor molecules.

precursor molecules per area is needed to saturate the surface. At the end of this process, two equal acetate-terminated surfaces are produced. This is schematically shown in Figure 2 for the [001] surface, with the groups taken from the reservoir highlighted in red. In practice, a symmetrical slab is constructed with sufficient layers to avoid any finite size effects.

Note that in this isodesmic³¹ surface formation reaction, the ratio of aromatic (*btc*) and aliphatic (*ac*) carboxylate groups changes for the exposed copper dimers. Potential stabilization effects on the Cu–O bond strength due to such local changes of the coordination environment are not captured by the force field. However, DFT calculations of carboxylate exchange reactions of model systems indicate that such effects can be neglected for the relative surface energies (Table S3 in the Supporting Information).

It is crucial to realize that for the HKUST-1 network in its *tbo* topology, different surfaces can be constructed for a given *hkl* plane. In Figure 3, all five surfaces considered in this work are shown by a line, indicating the slicing plane. For both [001] and [111], two surfaces can be constructed, which differ in the number of broken Cu–O bonds per surface area and accordingly in the density of acetate groups. These two cases are labeled by “a” and “b” in the following (Figure 3a,c). For the surfaces [111]a and [001]a, the least number of bonds have to be broken (see Figure 3); therefore, the number of both terminal acetate groups and free precursor molecules needed to saturate the surface is smallest. In Table 1, the density of additional paddle-wheel units taken from the precursor is given for all investigated surfaces. In this way, HKUST-1 surfaces are always generated with two acetate groups at each paddle-wheel unit in a *cis* arrangement. However, in the case of the [111]a surface, a distorted structure results, which is due to repulsive interactions of three adjacent *ac* groups, which are arranged

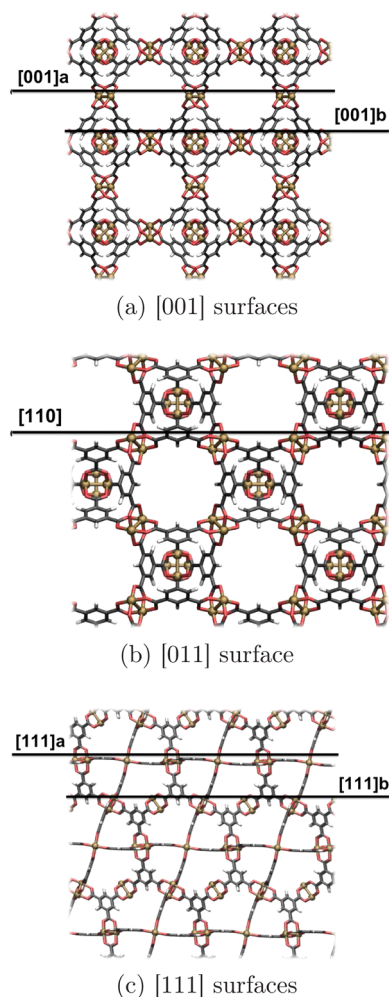


Figure 3. Possible surfaces to be generated by slicing through Cu–O bonds. For [001] and [111], two different surfaces denoted a and b can be generated with a different acetate density on the surface. The Figure shows a side view of the periodic system with a line indicating the slicing plane.

parallel to the surface (Figure 4). It is clear that under growth conditions, where an excess of free benzene-1,3,5-tricarboxylic acid molecules is present, these in-plane ac groups are likely to be replaced by one btc ligand to release the strain energy. It should be emphasized that for all others surfaces this additional ligand exchange reaction is not possible without constructing an acid-terminated surface, which can be excluded by the discussed IRRAS studies.³⁰ Therefore, to include this ligand exchange reaction at the [111]a surface, two additional molecular

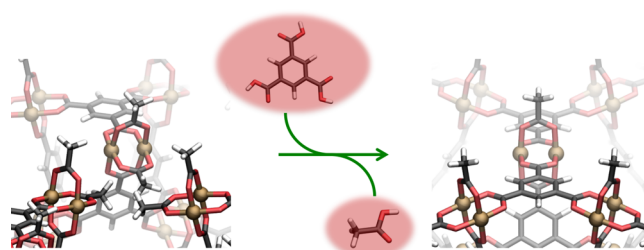


Figure 4. Ligand exchange reaction at the [111]a surface: Three ac groups are replaced by one btc ligand.

reservoirs for the free H₃btc and Hac molecules have to be considered, as shown in Figure 4.

The surface formation energies, ΔE_{surf} summarized in Table 1 represent the change in the strain energy when converting the bulk material to the acetate-terminated surface. It is calculated by

$$\Delta E_{\text{surf}} = \frac{1}{A} \left[E_{\text{slab}} - (E_{\text{bulk}} + nE_{\text{pw}}) + 2 \cdot nE_{\text{Hac}} - \frac{2 \cdot n}{3} E_{\text{H}_3\text{btc}} \right] \quad (2)$$

where E_{bulk} and E_{slab} are the energies calculated for the bulk and slab structure (normalized to the same number of formula units), E_{pw} is the MM energy of a single Cu₂(ac)₄ precursor, and A is the total surface area produced by the slicing. Here n is the number of precursor molecules needed so that $\rho_{\text{pw}} = (n/A)$. The last two terms E_{Hac} and $E_{\text{H}_3\text{btc}}$, which are only included in the case of the [111]a surface, represent the calculated energies of one benzene-1,3,5-tricarboxylic acid molecule and one acetic acid molecule. The calculated formation energies indicate an only modest relaxation of the network at the surface (see also Figure S2 in the Supporting Information). In the case of [001]b, the most dense layer of acetate groups at the surface leads to a weak dispersive stabilization compared with the other surfaces (see Figure S3 in the Supporting Information). However, in contrast with hard solids, where dangling bonds can lead to large surface relaxations, only the additional exchange reaction at the [111]a surface allows the interfacial structure to relax and release the strain energy.

To get a more realistic picture of the most favorable HKUST-1 surface termination, it is necessary to consider the free energies of surface formation. It can be assumed that vibrational degrees of freedom have a constant phase space volume during the reaction and can be ignored. Thus, only the translational entropy of the free acetate precursor has been included by means of the Sackur–Tetrode formula. The surface free energies ΔG_{surf} are given in Table 1 at different temperatures and concentrations of the metal precursor.

Table 1. Calculated Surface Energies ΔE_{surf} Relative to the [111]a Surface and Density of Paddle-Wheel Groups ρ_{pw} for All Considered Surfaces^a

surface	ρ_{pw} [groups nm ⁻²]	ΔE_{surf} [kcal mol ⁻¹ nm ⁻²]	ΔG_{surf} [kcal mol ⁻¹ nm ⁻²]		
			$T = 300, c = 0.01$	$T = 300, c = 0.1$	$T = 400, c = 0.1$
[001]a	0.57	1.57	5.78	5.37	6.70
[001]b	1.15	1.40	9.61	8.80	11.43
[011]	0.81	1.90	7.77	7.20	9.06
[111]a	0.50	0.00 (1.72) ^b	0.00	0.00	0.00
[111]b	1.00	1.74	8.89	8.19	11.38

^aFree surface energies ΔG_{surf} are given for different temperatures T (in K) and precursor concentrations $c = [\text{Cu}_2(\text{ac})_4]$ (in mol L⁻¹) and relative to the [111]a surface. ^bValue in parentheses represents the relaxed surface energy before the exchange of the in-plane ac by btc ligands.

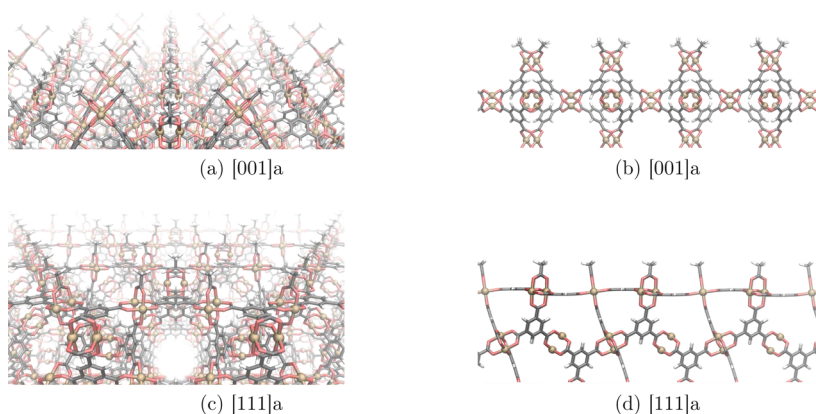


Figure 5. Perspective and side view of the most stable surfaces [001]a and [111]a.

The inclusion of the entropic contributions from the free copper precursors and the free carboxylic acids leads in most cases to a significantly endergonic free energy of surface formation. This observation and the correspondingly small surface formation energies corroborate that the formation of bulk HKUST-1 is an entropically driven process. The [111]a surface is thermodynamically most stable due to its lowest acetate density and because of the additional entropy gain by the ligand exchange reaction (Figure 4). In agreement with the experimental observation, we obtain an octahedral crystal morphology based on the Wulff construction^{32,33} using the calculated ΔG_{surf} (see Figure S4 in the Supporting Information).

Furthermore, our results explain the experimental observation that during one growth cycle of HKUST-1 a layer of half a unit cell is deposited.^{22,34} For both the [111] and the [001] surfaces the [111]a and the [001]a surface termination is more stable than the corresponding [111]b and [001]b cases, respectively, with the a-slicing planes separated by half the corresponding cell parameter (Figure 3a,c). In Figure 5, the two most stable surface terminations are shown in an overview. Note that the surfaces differ not just in the density of acetate groups but also in their orientation. In the most stable [111]a case, a single acetate group per paddle wheel is oriented perpendicular to the surface, whereas for [001]a the two acetate groups per paddle wheel are tilted (Figure 5b,d). Recently, Umemura et al. could show that with long-chain aliphatic acids as modulators, the crystal morphology can be converted to a cubic shape, indicating a higher stability for the [001] surface at high “modulator” concentrations.³⁵ Obviously, attractive interactions between such long-chain carboxylates benefit from the inclined orientation similar to aliphatic thiols in SAMs.^{36,37} Somewhat analog, this tilting could explain the [001] surface to interface preferentially to the tilted acetate-terminated SAMs in the oriented growth of HKUST-1 (see Figure 1).^{9,38}

In this work, to our knowledge for the first time, the atomistic structure of the surface termination of an archetypical MOF has been determined by theoretical methods. The surface of such soft crystals is conceptually different from hard solids like oxides. Because of the molecular nature, the truncation takes place along the weakest coordination bond of the framework, and the unsaturated sites are coordinated by donating ligands. In the case of the here-investigated HKUST-1, the termination of the surface by acetate groups appears reasonable. Formation energies of different crystal surfaces were

computed by combining strain energies from a first-principles parametrized force field with DFT reaction energies of model systems and thermodynamic contributions for taking saturating groups from a precursor reservoir. The results clearly show that the MOF formation is mainly an entropically driven process. Also, the strain energies of different surfaces are rather small, whereas entropic factors dominate the surface stability, making the [111] surface to be most stable, as experimentally observed. This is, however, only the first step toward a complete theoretical investigation of MOF surface and interface formation because other surface terminations and solvation effects will have to be considered. We are currently extending our approach in this respect also to obtain a molecular level insight into the effect of modulators and the oriented growth of HKUST-1 on functionalized SAMs.

■ ASSOCIATED CONTENT

Supporting Information

List of used force-field parameter sets and computational details. This material is available free of charge via the Internet at <http://pubs.acs.org>.

■ AUTHOR INFORMATION

Corresponding Author

*E-mail: rochus.schmid@rub.de.

Present Addresses

[†]S.A.: Physical Institute and Center for Nanotechnology (CeNTech), Westfälische Wilhelms-Universität Münster, 48149 Münster, Germany.

[‡]M.T.: Institut für Physikalische und Theoretische Chemie, Julius-Maximilians-Universität Würzburg, 97074 Würzburg, Germany.

Notes

The authors declare no competing financial interest.

■ ACKNOWLEDGMENTS

The German Science Foundation is acknowledged for financial support of this project within priority project SPP-1362 and SFB-558. S.A. is grateful to the Fonds der Chemischen Industrie for a stipend and the graduate school within SFB-558 for a scholarship. We thank Prof. Christof Wöll and Prof. Roland A. Fischer for motivating and helpful discussions.

REFERENCES

- (1) Rowsell, J. L. C.; Yaghi, O. M. Metal-Organic Frameworks: A New Class of Porous Materials. *Microporous Mesoporous Mater.* **2004**, *73*, 3–14.
- (2) Kitagawa, S.; Kitaura, R.; Noro, S. Functional Porous Coordination Polymers. *Angew. Chem., Int. Ed.* **2004**, *43*, 2334–2375.
- (3) Ferey, G. Hybrid Porous Solids: Past, Present, Future. *Chem. Soc. Rev.* **2008**, *37*, 191–214.
- (4) Li, Y.-S.; Liang, F.-Y.; Bux, H.; Feldhoff, A.; Yang, W.-S.; Caro, J. Molecular Sieve Membrane: Supported Metal-Organic Framework with High Hydrogen Selectivity. *Angew. Chem., Int. Ed.* **2010**, *49*, 548–551.
- (5) Shah, M.; McCarthy, M. C.; Sachdeva, S.; Lee, A. K.; Jeong, H.-K. Current Status of Metal-Organic Framework Membranes for Gas Separations: Promises and Challenges. *Ind. Eng. Chem. Res.* **2012**, *51*, 2179–2199.
- (6) Yazaydin, A. Ö.; Snurr, R. Q.; Park, T.-H.; Koh, K.; Liu, J.; LeVan, M. D.; Benin, A. I.; Jakubczak, P.; Lanuza, M.; Galloway, D. B.; et al. Screening of Metal-Organic Frameworks for Carbon Dioxide Capture from Flue Gas Using a Combined Experimental and Modeling Approach. *J. Am. Chem. Soc.* **2009**, *131*, 18198–18199.
- (7) Zacher, D.; Schmid, R.; Wöll, C.; Fischer, R. A. Surface Chemistry of Metal-Organic Frameworks at the Liquid-Solid Interface. *Angew. Chem., Int. Ed.* **2011**, *50*, 176–199.
- (8) Chui, S. S. Y.; Lo, S. M. F.; Charmant, J. P. H.; Orpen, A. G.; Williams, I. D. A Chemically Functionalizable Nanoporous Material $[\text{Cu}_3(\text{TMA})_2(\text{H}_2\text{O})_3]_n$. *Science* **1999**, *283*, 1148–1150.
- (9) Biemmi, E.; Scherb, C.; Bein, T. Oriented Growth of the Metal Organic Framework $\text{Cu}_3(\text{BTC})_2(\text{H}_2\text{O})_3 \cdot x\text{H}_2\text{O}$ Tunable with Functionalized Self-Assembled Monolayers. *J. Am. Chem. Soc.* **2007**, *129*, 8054–8055.
- (10) Shekhah, O.; Wang, H.; Kowarik, S.; Schreiber, F.; Paulus, M.; Tolan, M.; Sternemann, C.; Evers, F.; Zacher, D.; Fischer, R. A.; et al. Step-by-Step Route for the Synthesis of Metal Organic Frameworks. *J. Am. Chem. Soc.* **2007**, *129*, 15118–15119.
- (11) Shekhah, O.; Wang, H.; Zacher, D.; Fischer, R. A.; Wöll, C. Growth Mechanism of Metal-Organic Frameworks: Insights into the Nucleation by Employing a Step-by-Step Route. *Angew. Chem., Int. Ed.* **2009**, *48*, 5038–5041.
- (12) Diring, S.; Furukawa, S.; Takashima, Y.; Tsuruoka, T.; Kitagawa, S. Controlled Multiscale Synthesis of Porous Coordination Polymer in Nano/Micro Regimes. *Chem. Mater.* **2010**, *22*, 4531–4538.
- (13) Shoaee, M.; Anderson, M.; Attfield, M. Crystal Growth of the Nanoporous Metal-Organic Framework HKUST-1 Revealed by in Situ Atomic Force Microscopy. *Angew. Chem., Int. Ed.* **2008**, *47*, 8525–8525.
- (14) Biemmi, E.; Darga, A.; Stock, N.; Bein, T. Direct Growth of $\text{Cu}_3(\text{BTC})_2(\text{H}_2\text{O})_3 \cdot x\text{H}_2\text{O}$ Thin Films on Modified QCM-Gold Electrodes - Water Sorption Isotherms. *Microporous Mesoporous Mater.* **2008**, *114*, 380–386.
- (15) Hinterholzinger, F.; Scherb, C.; Ahnfeldt, T.; Stock, N.; Bein, T. Oriented growth of the functionalized metal-organic framework CAU-1 on -OH- and -COOH-terminated self-assembled monolayers. *Phys. Chem. Chem. Phys.* **2010**, *12*, 4515–4520.
- (16) Schoedel, A.; Scherb, C.; Bein, T. Oriented Nanoscale Films of Metal-Organic Frameworks By Room-Temperature Gel-Layer Synthesis. *Angew. Chem., Int. Ed.* **2010**, *49*, 7225–7228.
- (17) Scherb, C.; Williams, J. J.; Hinterholzinger, F.; Bauer, S.; Stock, N.; Bein, T. Implementing Chemical Functionality into Oriented Films of Metal-Organic Frameworks on Self-Assembled Monolayers. *J. Mater. Chem.* **2011**, *21*, 14849–14856.
- (18) Hinterholzinger, F. M.; Wuttke, S.; Roy, P.; Preuß, T.; Schaate, A.; Behrens, P.; Godt, A.; Bein, T. Highly Oriented Surface-Growth and Covalent Dye Labeling of Mesoporous Metal-Organic Frameworks. *Dalton Trans.* **2012**, *41*, 3899–3901.
- (19) Shoaee, M.; Agger, J. R.; Anderson, M. W.; Attfield, M. P. Crystal Form Defects and Growth of the Metal Organic Framework HKUST-1 Revealed by Atomic Force Microscopy. *CrystEngComm* **2008**, *10*, 646–648.
- (20) Cubillas, P.; Anderson, M. W.; Attfield, M. P. Crystal Growth Mechanisms and Morphological Control of the Prototypical Metal-Organic Framework MOF-5 Revealed by Atomic Force Microscopy. *Chem.—Eur. J.* **2012**, *18*, 15406–15415.
- (21) Attfield, M. P.; Cubillas, P. Crystal Growth of Nanoporous Metal Organic Frameworks. *Dalton Trans.* **2012**, *41*, 3869–3878.
- (22) John, N. S.; Scherb, C.; Shoaee, M.; Anderson, M. W.; Attfield, M. P.; Bein, T. Single Layer Growth of Sub-Micron Metal-Organic Framework Crystals Observed by in Situ Atomic Force Microscopy. *Chem. Commun.* **2009**, 6294–6296.
- (23) Reuter, K.; Scheffler, M. Composition, Structure, And Stability of $\text{RuO}_2(110)$ as a Function of Oxygen Pressure. *Phys. Rev. B* **2001**, *65*, 035406.
- (24) Tafipolsky, M.; Amirjalayer, S.; Schmid, R. First-Principles-Derived Force Field for Copper Paddle-Wheel-Based Metal-Organic Frameworks. *J. Phys. Chem. C* **2010**, *114*, 14402–14409.
- (25) Amirjalayer, S.; Tafipolsky, M.; Schmid, R. Exploring Network Topologies of Copper Paddle Wheel Based Metal-Organic Frameworks with a First-Principles Derived Force Field. *J. Phys. Chem. C* **2011**, *115*, 15133–15139.
- (26) Cossi, M.; Rega, N.; Scalmani, G.; Barone, V. Energies, Structures, And Electronic Properties of Molecules in Solution with the C-PCM Solvation Model. *J. Comput. Chem.* **2003**, *24*, 669–681.
- (27) Barone, V.; Cossi, M. Quantum Calculation of Molecular Energies and Energy Gradients in Solution by a Conductor Solvent Model. *J. Phys. Chem. A* **1998**, *102*, 1995–2001.
- (28) Srivastava, G. P. Theory of Semiconductor Surface Reconstruction. *Rep. Prog. Phys.* **1997**, *60*, 561–613.
- (29) Odbadrakh, K.; Lewis, J. P.; Nicholson, D. M.; Petrova, T.; Michalkova, A.; Leszczynski, J. Interactions of Cyclotrimethylene Trinitramine (RDX) with Metal Organic Framework IRMOF-1. *J. Phys. Chem. C* **2010**, *114*, 3732–3736.
- (30) Zybalyo, O.; Shekhah, O.; Wang, H.; Tafipolsky, M.; Schmid, R.; Johannsmann, D.; Wöll, C. A Novel Method to Measure Diffusion Coefficients in Porous Metal-Organic Frameworks. *Phys. Chem. Chem. Phys.* **2010**, *12*, 8093–8098.
- (31) To compute energy differences with (nonreactive) MM force fields, it is necessary to perform isodesmic reactions without changes in the number and nature of the bonds to make a valid comparison between two configurations on the same potential energy surface.
- (32) Wulff, G. Velocity of Growth and Dissolution of Crystal Faces. *Z. Kristallogr.* **1901**, *34*, 449–530.
- (33) Herring, C. Some Theorems on the Free Energies of Crystal Surfaces. *Phys. Rev.* **1951**, *82*, 87–93.
- (34) Munuera, C.; Shekhah, O.; Wang, H.; Wöll, C.; Ocal, C. The Controlled Growth of Oriented Metal-Organic Frameworks on Functionalized Surfaces As Followed by Scanning Force Microscopy. *Phys. Chem. Chem. Phys.* **2008**, *10*, 7257–7261.
- (35) Umehara, A.; Diring, S.; Furukawa, S.; Uehara, H.; Tsuruoka, T.; Kitagawa, S. Morphology Design of Porous Coordination Polymer Crystals by Coordination Modulation. *J. Am. Chem. Soc.* **2011**, *133*, 15506–15513.
- (36) Ulman, A. Formation and Structure of Self-Assembled Monolayers. *Chem. Rev.* **1996**, *96*, 1533–1554.
- (37) Love, J. C.; Estroff, L. A.; Kriebel, J. K.; Nuzzo, R. G.; Whitesides, G. M. Self-Assembled Monolayers of Thiolates on Metals as a Form of Nanotechnology. *Chem. Rev.* **2005**, *105*, 1103–1170.
- (38) Zacher, D.; Shekhah, O.; Wöll, C.; Fischer, R. A. Thin Films of Metal-Organic Frameworks. *Chem. Soc. Rev.* **2009**, *38*, 1418–1429.